Copyright ⓒ 2024 KSII

Link Quality Enhancement with Beamforming Using Kalman-based Motion Tracking for Maritime Communication

Kyeongjea Lee[1], Joo-Hyun Jo[1], Sungyoon Cho[2], Kiwon Kwon[2] and Dong Ku Kim[1*]
[1] Department of Electrical engineering, Yonsei University Seoul, South Korea
[2] Smart Network Research Center, Korea Electronics Technology Institute Seoul, South Korea
[e-mail: kjlee92@yonsei.ac.kr, joohyun_jo@ yonsei.ac.kr, sycho@keti.re.kr, kwonkw@keti.re.kr, dkkim@yonsei.ac.kr]
*Corresponding author: Dong Ku Kim

Received January 12, 2024; revised April 26, 2024; accepted May 29, 2024; published June 30, 2024

Abstract

Conventional maritime communication struggles to provide high data rate services for Internet of Things (IoT) devices due to the variability of maritime environments, making it challenging to ensure consistent connectivity for onboard sensors and devices. To resolve this, we perform mathematical modeling of the maritime channel and compare it with real measurement data. Through the modeled channel, we verify the received beam gain at buoys on the ocean surface. Additionally, leveraging the modeled wave motions, we estimate future angles of the buoy to use the Extended Kalman Filter (EKF) for design beamforming strategies that adapt to the evolving maritime environment over time. We further validate the effectiveness of these strategies by assessing the results from an outage probability perspective. focuses on improving maritime communication by developing a dynamic model of the maritime channel and implementing a Kalman filter-based buoy motion tracking system. This system is designed to enable precise beamforming, a technique used to direct communication signals more accurately. By improving beamforming, the aim is to enhance the quality of communication links, even in challenging maritime conditions like rough seas and varying sea states. In our simulations that consider realistic wave motions, you've observed significant improvements in link quality due to the enhanced beamforming technique. These improvements are particularly notable in environments with high sea states, where communication challenges are typically more pronounced. The progress made in this area is not just a technical achievement; it has broad implications for the future of maritime communication technologies. This paper promises to revolutionize the way we approach communication in maritime environments, paving the way for more reliable and efficient information exchange on the seas.

Keywords: Maritime Communication, Beamforming, Channel modeling, Internet of things (IoT), Extended Kalman filter, Motion tracking.

This research was a part of the project titled 'The advancement of smart aids to navigation facilities (20210636)', funded by the Ministry of Oceans and Fisheries, Korea.
A preliminary version of this paper was presented at APIC-IST 2023, and was selected as an outstanding paper.

http://doi.org/10.3837/tiis.2024.06.013 **ISSN : 1976-7277**

1. Introduction

The rapid advancement of the IoT and the evolution of 6 generation(6G), there is a noticeable acceleration in the advancement of communication technologies. This progress is driving the expansion of communication capabilities, particularly within the maritime domain [1],[2]. However, maritime communication has not progressed at the same pace as terrestrial systems. Addressing the discrepancy in this inequality takes on significance as maritime activities continue to rise. With an increasing need for dependable connectivity in oceanic settings, there is a growing demand for proficient communication systems. These systems are designed to provide excellent communication services, offering extensive coverage across the oceanic expanse, as highlighted in [3–6]. Unlike terrestrial channels, the oceanic unique environment of maritime communication scenarios stated in [3] such as ocean waves and wind keep buoys of small and medium size heaving and tilting, which makes it difficult to maintain a stable link between a base station and buoys. The challenges presented by factors such as ocean waves and wind make maintaining a stable link connection paramount, as highlighted in [7]. Recognizing this pressing necessity, our research is dedicated to bridging the technological gaps in oceanic communication, with the goal of establishing a robust infrastructure for the maritime sector. A fundamental element in achieving this resilience lies in the communication models that underpin system design and functionality. However, many prevailing studies in maritime communication heavily rely upon the Rician channel model approximation, as mentioned in [8],[9]. Unfortunately, this often results in overlooking the dynamic movements of maritime objects and the continuous fluctuations within communication channels. Moving towards enhanced precision in modeling, particularly in terms of accounting for real-time behaviors and variations in communication channels, will play a critical role in developing systems that are suitably equipped to tackle the intricacies of maritime communication challenges. Furthermore, as mentioned in [10], conventional communication systems used in maritime settings have faced significant difficulties stemming from the ever-changing and unpredictable conditions of the ocean environment. A notable constraint has arisen due to the absence of beamforming and beam-tracking techniques, as indicated in [11]. Reference [12–16] introduced beam tracking in terrestrial communications. The absence of these techniques can result in compromised link quality for maritime communication systems. By integrating beamforming [17] and beam tracking capabilities, the potential exists to enhance signal directionality and concentration, thereby establishing more dependable communication across water bodies. Recognizing these challenges underscores the significance of investigating beamforming and beam-tracking within maritime scenarios, as highlighted in [18]. We introduce a more detailed and precise channel model that considers the actual dynamics of maritime objects and channel variations, moving beyond the conventional Rician model. This provides a more accurate representation of real-world marine conditions. Furthermore, we propose a novel algorithm that optimizes both beamforming and beam tracking in real-time maritime scenarios. This algorithm has demonstrated superior performance in terms of signal strength and reliability when compared to existing solutions. This amalgamation aspires to offer not just a reactive maritime communication system but a proactive one. In Section 2 of this thesis, we elaborate on the channel model for the proposed maritime Multiple Input Multiple Output (MIMO) communication system using buoys. In Section 3, we present a protocol for the beam misalignment compensation, based on the sensors in smart devices In Section 4, we present the simulation result. In section 5, We summarize our conclusions in this paper. In summary, the suggested MIMO Maritime communication system for buoys could significantly improve the reliability.

2. System model

In this section, we consider a maritime communication system for a downlink scenario. In the considered scenario, the buoy and base station (BS) employ M and N antennas, respectively. The overall maritime system architecture is shown in **Fig. 1**. In the near-shore communication link from the BS to buoy, the direct path will be most prevalent. As a result, we consider an empirical Rician fading model. Then, the received signal, denoted as $\mathbf{y} \in \mathbb{C}^{N \times 1}$, at the buoy can be represented as:

$$\mathbf{y} = \mathbf{F}_{\mathrm{r}}\mathbf{H}_{\mathrm{R}}^{\mathrm{H}}\mathbf{F}_{\mathrm{t}}s + \mathbf{n}, \tag{1}$$

where $\mathbf{F}_{\mathrm{r}} \in \mathbb{C}^{N\times N}$, $\mathbf{F}_{\mathrm{t}} \in \mathbb{C}^{M\times M}$ are the received beamformer at the buoy and transmit beamformer at BS. We assume that the base station has precise knowledge of the buoy's location, the transmission precoding is omitted. The transmit signal s is for the buoy and with a normalized power $\mathbb{E}(\mathrm{ss}^{\mathrm{H}}) = \mathbf{I}$. During data transmission, a single data stream is utilized at a time, indicating that data is sent using only one continuous flow of information at any given moment. The noise vector $\mathbf{n} \in \mathbb{C}^{\mathrm{N}\times 1}$ follows an additive white Gaussian noise (AWGN) distribution with covariance matrix $\sigma^2\mathbf{I}$, where σ^2 is the noise variance and $\mathbf{I}$ is the identity matrix. $\mathbf{H}_{\mathrm{R}} \in \mathbb{C}^{\mathrm{M}\times\mathrm{N}}$ is the Rician fading channel from the BS to buoy, and it can be represented as follows:

$$\mathbf{H}_{\mathrm{R}} = \sqrt{\frac{K}{K+1}} \times \mathbf{H}_{\mathrm{LOS}} + \sqrt{\frac{1}{K+1}} \times \mathbf{H}_{\mathrm{NLOS}}, \tag{2}$$

where $\mathrm{H}_{\mathrm{LOS}} = \exp(1j \times \emptyset)$ is the LoS component. $\emptyset \sim U(0,2\pi)$ denotes a uniform distribution in the range $(0,2\pi)$. $\mathrm{H}_{\mathrm{NLOS}} = \frac{X+1jY}{\sqrt{2}}$ is the LoS component. $X \sim \mathcal{N}(0,1)$ and $Y \sim \mathcal{N}(0,1)$ are the real and imaginary numbers, respectively. Those represent a normal distribution with a mean of 0 and a variance of 1.

2.1 Mathematical derivation of angle of buoy in maritime communication

In the received signal of (1), the line of sight (LoS) path within the Rician channel model $\mathbf{H}_{\mathrm{R}}$ includes a significant factor related to the angle of arrival for the LoS path. Thereby, to faithfully evaluate the communication capability of the buoy in the maritime scenario, understanding the complex mechanisms of fluid dynamics in ocean waves and the variations in surface elevation in highly dynamic oceanic environments is crucial. We first examine and delve into the mathematical aspects of the buoy's movement and how the channel changes due to fluctuations in the wave surface. Based on the Bretschneider spectrum model, as mentioned in [19], the spectrum model for the open ocean wave is given by:

$$S(\omega) = \frac{5}{16}\frac{H_s^2\omega_p^4}{\omega^5} exp\left(-\frac{5}{4}\left(\frac{\omega_p}{\omega}\right)^4\right) \ \frac{m^2}{\frac{rad}{s}}, \tag{3}$$

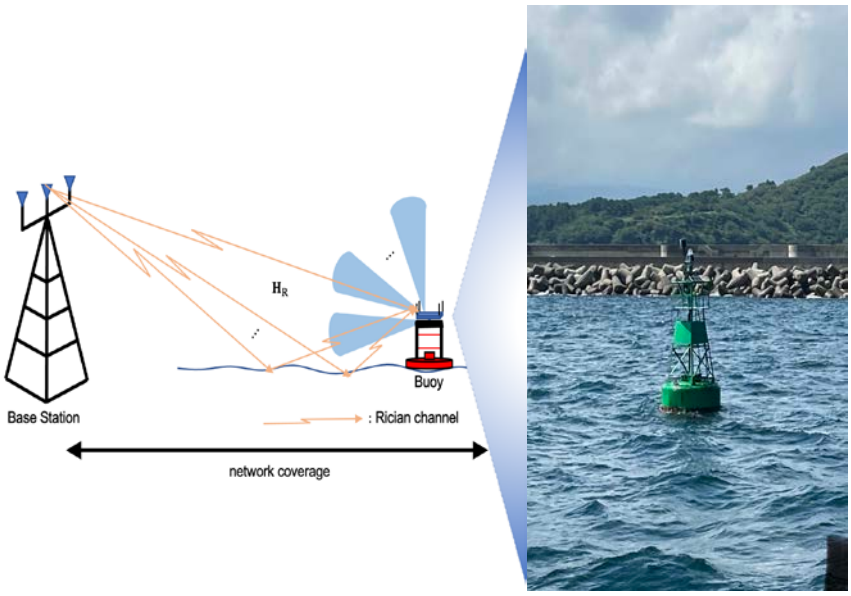

Fig. 1. System architectures

where $\boldsymbol{H_s}$, $\boldsymbol{\omega}$ and $\boldsymbol{\omega_p}$ represent the height of the wave, angular frequency, and peak angular frequency, respectively. Here, the peak period of the peak angular frequency is denoted as $T_p = 2\pi/\omega_p$. With the spectrum model of (2), to obtain the amplitude of the wave involving the multiple wave components, we further assume that the amplitude of each wave components follows the Rayleigh distribution as referred in [20]. Then, the elevation denoted as $\gamma(x,t)$ of the wave components at time *t* and position *x* can be expressed as follows:

$$\gamma(x,t) = \sum_{i=1}^{N_f} a_i \cos(2\pi f_i t + k_i x + \alpha_i), \tag{4}$$

where N_f and α_i are the number of wave components and the phase for the i-th frequency f_i, respectively. The wave number k_i is determined by w_i^2/g, where g is the acceleration of gravity. Here, the expected amplitude of each frequency component, represented by $\mathrm{E}[a_i]$, can be computed as follows [21]:

$$\mu_i = \sqrt{2 * S(\omega_i) * \Delta\omega}, \tag{5}$$

where $\Delta\omega$ is the frequency interval of the spectrum $\mathrm{S}(\omega_i)$. It is noted that the wave's elevation formulated by (3) provides a more accurate model to address the motions of the buoy and faithfully capture the characteristics of the practical channel model in maritime communications. We now investigate the buoy angle in terms of the wave's elevation in (3). It shows that the dynamic angle of the buoy can be determined by the geometric structure as depicted in **Fig. 2**. Upon observing in **Fig. 2**, it becomes evident that 'heaving' and 'tilting' constitute the motion. Because of this movement, the horizontal beam of the receiving beamforming remains stationary, while the vertical beam undergoes motion. Therefore, it is essential to elucidate this phenomenon. As the sea level obtained by (3) changes, the antenna direction with respect to the elevation of zero varies. Thereby, the buoy's angle with Angle of

Arrival (AoA) is 0 denoted as Ω_0 can be obtained by the elevations at the time (t-1) and (t+1). Subsequently, the angle of the buoy is expressed as:

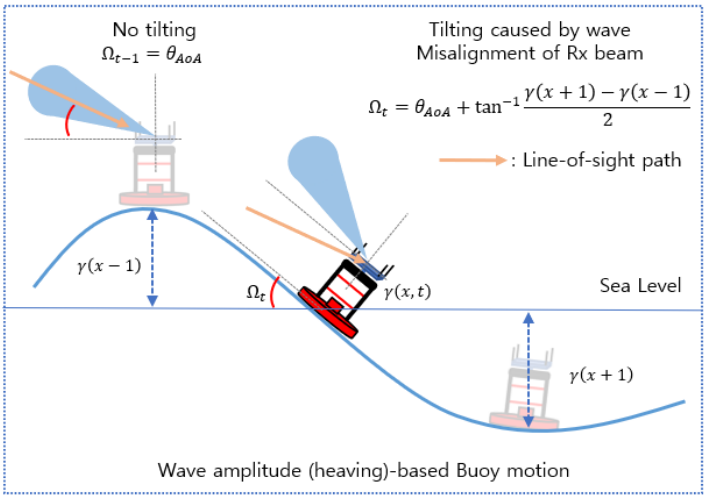

Fig. 2. Modeling the angle of a buoy in a dynamic marine environment

$$\boldsymbol{\Omega_0 = \tan^{-1}\left(\frac{\gamma(x,t+1)-\gamma(x,t-1)}{2}\right)}, \quad (6)$$

Equation (5) involves the practical wave elevation at the specific point x of the fixed buoy. To establish the Angle of Arrival(AoA) of the LoS path of the Rician channel model in (1) as time varies, this mathematical modeling of the buoy's antenna direction is employed. This approach enables us to track changes in the angle over time, leading to a deeper comprehension of ocean wave behavior. **Fig. 3** validates the feasibility of the mathematical model (6), where the actual buoy's motion is obtained at the moderate ocean with a variable height of the wave and angular frequency. These Actual values of buoys are measured when the sea state was moderated by the Korean Ministry of Oceans and Fisheries, and the values obtained based on this data represent the actual angles of buoy movement. The actual values of the angle of the buoy movement indicate that the average angle is 0.4 degrees, and the variance is 8.8 degrees. Through mathematical modeling for a moderate sea state level, the average movement angle of the buoy is about 0.3 degrees, and the variance is about 8.9 degrees. Mathematical modeling of the moving angle of the buoy is used to construct a time-varying channel. It is noted that the formulated AoA model. This evaluation confirms the reasonableness of the formulated AoA model (6), namely, the relaxations employed in the derived outcome.

3. The proposed method

Fig. 4 depicts the equivalent channel gain received at the buoy considering the oceanic channel. This shows that it is not consistently advantageous to change the received beamforming constantly and demonstrates that location information is available. It is only when the gain falls notably below a set threshold that adjusting the beamforming becomes relevant. Continually tweaking beamforming from a communications standpoint adds undue intricacy and can lead to lags due to regular recalculations. Moreover, if the received signal quality remains above an acceptable threshold, there's minimal to no discernible benefit in making

those adjustments. Only when the gain falls below our defined threshold is there a tangible advantage to refining the beamforming, as it can considerably restore and enhance the link

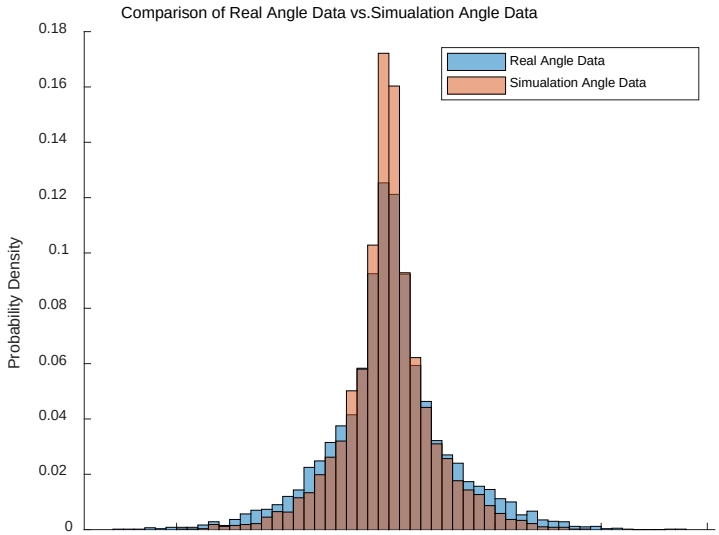

Fig. 3. Compare simulation angle data Ω with real angle data variation over time (Sea state level 4)

quality. This adaptive strategy not only ensures robust communication but also optimizes system resources by focusing on adjustments only when truly necessary.

3.1 Initial beam searching

The foundation for this adjustment is to determine the initial beam for the highest beam gain based on the initial AoA (θ_{n}) of the received signal. Through these, we can formulate the beam sweeping at buoy as follows [22]:

$$\boldsymbol{n}^{*} = \mathbf{arg\,max}_{\mathbf{n}} |\bar{\mathbf{F}}(\boldsymbol{\theta}_{\mathbf{AoA}})\mathbf{H}_{\mathbf{R}}|^{\mathbf{2}}, \tag{7}$$

By multiplying the channel matrix with the steering beamforming vector $\bar{\mathbf{F}}(\theta_{\mathrm{AoA}})$. Then, we can evaluate the resulting gains. From these, received beamforming vector with the highest gain is selected, allowing us to identify the initial beam direction to ensure maximum signal strength and performance.

3.2 Refinement and tracking

In maritime channels like **Fig. 2**, it can be readily noted that the heaving and tilting of buoys on ocean waves cause a misalignment of beamforming between BS and buoy that wouldn't have occurred in terrestrial channels. To enhance the link reliability, The buoy adjusts its receiving beam autonomously using the estimated angles. In our study, we delve into the functionalities and distinctions between the Kalman Filter (KF) and the Extended Kalman Filter (EKF), highlighting their pivotal roles in dynamic state estimation and prediction. The KF is particularly efficient in environments characterized by linear models and Gaussian noise, making it an excellent choice for straightforward tracking and navigation tasks. However, the Extended Kalman Filter comes into its own in more complex scenarios due to its capacity to handle nonlinear dynamics. This is achieved through a linearization process, where the EKF approximates the nonlinear behaviors of a system using linear models, thereby allowing for

more accurate predictions in situations where traditional linear models fail. The applicability of these filters extends significantly into maritime communications, particularly in beamforming technologies where precise signal direction and management are crucial. In dynamic maritime environments, where the conditions are unpredictable and often nonlinear, the EKF's ability to adapt and predict beam directions is invaluable. By utilizing the Extended Kalman Filter, it can enhance the efficiency and accuracy of beamforming techniques. This improvement is critical for maintaining robust communication links in maritime settings, ensuring that signal strength and clarity are maximized even under challenging conditions. Therefore, in this paper, we implemented the Extended Kalman Filter to advance the application of beamforming in maritime communication, showcasing its effectiveness in managing the complexities associated with this advanced technology. we next show how this mismatch could be overcome via a phase rotation operation using an Kalman filter [23],[24]. Before use EKF, we must set the angle the buoy:

$$B_t = \begin{bmatrix} \Omega_t \\ \tau_t \end{bmatrix}, \tag{8}$$

where Ω_t and τ_t is angle and velocity of buoy. We now use the elevation value, so the measurement model H can be expressed to:

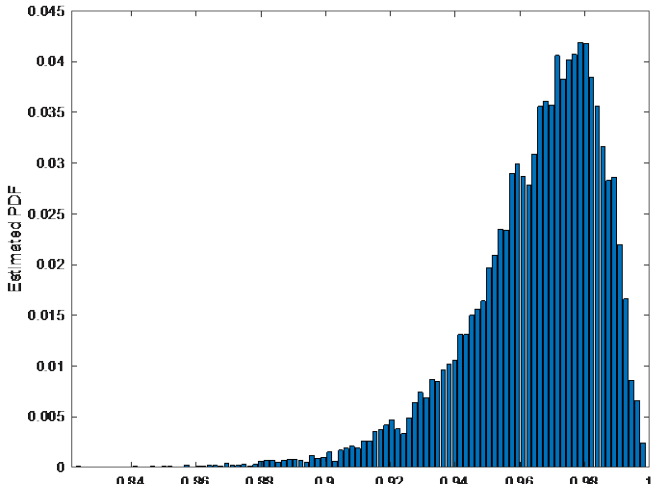

Fig. 4. Probability density function of equivalent channel gain (Sea state 4)

$$H = \left[\frac{\partial}{\partial \Omega} \arctan\left(\frac{\gamma(\mathrm{x},\ t) - \gamma(x, t-1)}{2}\right), 0\right], \tag{9}$$

This is non-linear system. Therefore, we compute the Jacobian matrix for the behavioral and measurement models of the system. For the behavioral model, the Jacobian will be a unit matrix since the system depends primarily on changes in state (i.e., elevation). However, in real-world situations, we rarely know the behavioral model exactly. For the measurement model, we use the change in elevation with respect to Ω, this Jacobian will contain the partial derivative of elevation with respect to Ω.

$$H_t = H(\Omega_{t-1}) + \frac{\Omega H}{d\Omega}|_{\Omega_{t-1}}(\Omega - \Omega_{t-1}), \tag{10}$$

To use this parameter, it must go through a prediction process. We set the predicted state estimate as follow:

$$B_{t|t-1} = A_{t-1} * B_t, \tag{11}$$

where $B_{t|t-1}$is the predicted state of next time. Then, the predicted estimate covariance is as follow:

$$\mathrm{P}_{t|t-1} = A_t P_{t-1} A_t^H + Q_t, \tag{12}$$

where $\mathrm{P}_{t|t-1}$ represents the uncertainty of our prediction. Q_t is a process noise covariance matrix, accounting for the unpredictability in the state evolution. When a new measurement is available, the EKF updates its state estimate. The difference between the actual measurement and our predicted measurement (from the predicted state) is the residual:

$$y_t = B_t - H_t B_{t|t-1}, \tag{13}$$

where H_t maps the state to the measurement space. To account for uncertainties in our prediction and the measurement, we compute the residual covariance:

$$S_t = H_t \mathrm{P}_{t|t-1} H_t^H, \tag{14}$$

The Kalman gain, K_t is calculated next. This determines how much we should adjust our state prediction based on the new measurement:

$$K_t = P_{t|t-1} H_t S_t^{-1}, \tag{15}$$

The state estimate is then updated:

$$\hat{B}_t = B_{t|t-1} + K_t y_t, \tag{16}$$

Finally, we update our estimate's uncertainty:

$$\widehat{P_t} = (I - K_t H_t) P_{t|t-1}, \tag{17}$$

By iteratively performing prediction and update steps, the EKF offers a real-time estimation framework. For our system, it provides a way to estimate the angle and its angular velocity even in the presence of noisy measurements. We compare the angle estimated by EKF with the actual angle in **Fig. 5**. Through this methodology, the system can dynamically react to changes and continue to provide accurate estimates over time. We summarized the process in Algorithm 1. To proceed with Algorithm 1 as described below, constraints is as follows:

$$\hat{P}_{error} < \gamma(t)_{var}, \tag{18}$$

where $\hat{P}_{error}$ is a remaining uncertainty of the state vector resulting in remaining beamforming misalignment while $\gamma(t)_{var}$ is ocean wave variance resulting in beamforming misalignment

without tracking of time varying AoA due to motion of buoy, respectively. If the variation or inconsistency in tracking is greater than the variability of the sea state, the application of the EKF for estimation purposes may not be optimal. The fundamental reason behind this is that when tracking noise or variability is excessively high, it can overshadow or complicate the data, thus diminishing the effectiveness and predictive accuracy of the EKF. Given these considerations, it might be against relying on the EKF for estimation in scenarios where the tracking variation significantly surpasses that of the sea state.

Algorithm 1: EKF-based beam refinement method

Initialize: The angle and velocity of the buoy $B_t = \begin{bmatrix} \Omega_t \\ \tau_t \end{bmatrix}$, measurement model H_t,

state-transition model A_t predicted measurement residual $y_t = B_t - H_t B_{t|t-1}$

Step 1: Prediction

Predicted state estimate, $B_{t|t-1} = A_{t-1} * B_t$

Predicted estimate covariance $\mathrm{P}_{t|t-1} = A_t P_{t-1} A_t^H + Q_t$

Step 2: Update

Innovation. $y_t = B_t - H_t B_{t|t-1}$

$S_t = H_t \mathrm{P}_{t|t-1} H_t^H$

Kalman Gain $K_t = P_{t|t-1} H_t S_t^{-1}$

State Update $\widehat{B_t} = B_{t|t-1} + K_t y_t$

Covariance Update. $\widehat{P_t} = (I - K_t H_t) P_{t|t-1}$

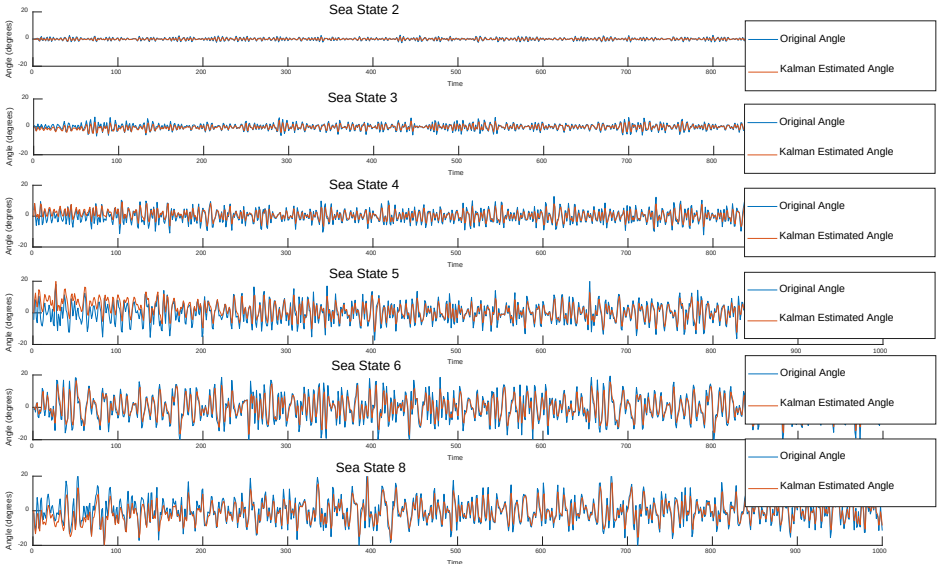

Fig. 5. Comparison of actual buoy movement angle Ω with Kalman data $\widehat{\Omega}$ over time according to Sea State

3.3 Link failure

In the event of a link failure or network outage, communication in specific areas could be disrupted. As a result, communication coverage would be compromised, leading to reduced efficiency. To address this challenge, it becomes imperative to establish contingency plans for link failures and network outages. These measures are essential for maintaining seamless communication coverage and optimizing operational effectiveness. Link failure is that if the

performance of the beam we have set is lower than the predefined threshold known, it is referred to as a link failure. The link failure inequality is as follows:

$$\left|\mathbf{F}_{\mathrm{k}[:,n^*]}\boldsymbol{\Phi}\left(\theta_{\mathrm{n}}+\widehat{\Omega}_t\right)\mathbf{H}_{\mathrm{R}}\right|^2<\varphi_{\mathrm{LF}}, \tag{19}$$

where φ_{LF} is the beam performance gain threshold that we configure. Therefore, we calculate the probability that the received gain becomes less than some threshold to get the outage. As described above, the initiation of a comprehensive beam adjustment procedure entails the initialization of the received signal y, establishment of a fixed beam F, and definition of a time duration T. Subsequent actions encompass the following steps. First, the base station and the buoy location is given information, it is assumed that the angle of arrival (AOA) is known. Consequently, the initial beamforming vector for the beamforming process is set as the steering vector with the highest gain, as follows:

$$n^*=\arg\max_{n\in S_N}\bar{\mathbf{F}}(\theta_{\mathrm{n}})\mathbf{H}_{\mathrm{R}}, \tag{20}$$

where n^* is constant of beamforming vector. Then, we refinement and tracking the beamforming to use estimate angle:

$$\widehat{\Omega}_t=\Omega_{\mathrm{t|t-1}}+K_t y_t, \tag{21}$$

Algorithm 2: Beam tracking method

Initialize: received signal y, Fixed beam F, Time duration T
For k = 1: K
  Step 1: Rough direction finding.
    Beam sweeping, $n^*=\arg\max_{n\in S_N}\bar{\mathbf{F}}(\theta_{\mathrm{n}})\mathbf{H}_{\mathrm{R}}$ in (7)
  Step 2: Refinement and tracking
    Sensing-based direction estimation, $\widehat{\Omega_{\mathrm{t}}}=\Omega_{\mathrm{t|t-1}}+K_t y_t$ in Algorithm 1
    Direction fine-tuning, $\theta_{\mathrm{n}}+\widehat{\Omega}_t$
 If $\left|F_{[:,n^*]}\boldsymbol{\Phi}\left(\theta_{\mathrm{n}}+\widehat{\Omega}_t\right)\mathbf{H}_{\mathrm{R}}\right|^2<\varphi_{\mathrm{LF}}$
  Go to Step 1
 Else
  Go to Step 2
End

Furthermore, we adjust the beam considering the direction fine-tuning factor, denoted as $\widehat{\Omega}_t$, based on the previously known AoA. The final calculated receive gain at the buoy is as follows:

$$g_k=\bar{\mathbf{F}}_{\mathrm{k}[:,n^*]}\boldsymbol{\Phi}\left(\theta_{\mathrm{n}}+\widehat{\Omega}_t\right)\mathbf{H}_{\mathrm{R}}, \tag{22}$$

In Eq. (22), $\bar{\mathbf{F}}_{\mathrm{k}[:,n^*]}$is the optimal beam where $\bar{\mathbf{F}}(\theta_{\mathrm{AoA}_{[n^*]}})$ is steering vector with the structure $\bar{\mathbf{F}}\left(\theta_{\mathrm{AoA}[\,n^*]}\right)=\left[1,e^{\mathrm{j}\pi\sin\theta_{\mathrm{AoA}n^*}},\ldots,e^{j(N-1)\pi\sin\theta_{\mathrm{AoA}n^*}}\right]^T$, $n=1,\ldots,N$. And $\boldsymbol{\Phi}(\theta_{\mathrm{n}}+\widehat{\Omega}_t)$ is the phase rotation of the original vector, where $\boldsymbol{\Phi}(\theta_{\mathrm{n}}+\widehat{\Omega}_t)$ is a diagonal matrix given by $\boldsymbol{\Phi}\left(\widehat{\Omega}_k\right)=\mathrm{diag}\{1,e^{j\theta_{\mathrm{n}}+\widehat{\Omega}_t},\ldots,e^{j(N-1)\theta_{\mathrm{n}}+\widehat{\Omega}_t}\}$ and $\widehat{\Omega}_t$ is the corresponding shifted phase that varies from $-\pi/\mathrm{N}$ to π/N. Finally, we proceed with the process of beam adjustment as follows: If the received beam gain is lower than the threshold for link failure according to the inequality expressed in the following equation:

$$\left|\bar{\mathbf{F}}_{[:,n^*]}\boldsymbol{\Phi}\left(\theta_{\mathrm{n}}+\widehat{\Omega}_t\right)\mathbf{H}_{\mathrm{R}}\right|^2<\varphi_{\mathrm{LF}}, \tag{23}$$

We initiate the process of searching for and readjusting the beam. Conversely, if the received beam gain is greater than the threshold, we perform beam adjustment alone. Based on the above steps, the entire process is summarized in Algorithm 2. We verify the performance in simulation based on the received beam gain at the buoy.

4. Simulation

In this section, numerical results are provided for the outage probability according to beamforming algorithm and the sea state of the ocean. We consider a maritime communication system network illustrated in **Fig. 1**, in which BS and buoy are equipped with multi antennas. The Automatic Identification System (AIS) maritime system operates within the frequency band of 1.7GHz, and the reason for utilizing a K-factor of 3 is rooted in the conventional application of the two-ray channel model in maritime channel scenarios [7]. Then, in maritime communication scenarios, it is customary to consider a base station's transmission power of 46 dBm. This choice aligns with the typical consideration of such scenarios in the maritime channel modeling context. The system parameters are summarized in **Table 1**.

Table 1. Simulation parameter.

Parameters	Values
Center Frequency	1.7 GHz
K-factor	3
Distance	10 km
Gravity Acceleration	9.8 $\mathrm{m/s^2}$
BS power	46 dBm
Sea state level	Level 2,3,4,5,6

Fig. 6 evaluates the beamforming methods in the maritime communication scenario, where blue, red, and yellow lines are EKF-based beam tracking with beam-switching in Algorithm 2, without beam-switching in Algorithm 1, and fixed initial beamformer in (7), respectively. In **Fig. 6(a)**, where the number of bouy's antennas is four, the EKF algorithm is always superior to other method in the whole region of sea state level due to the tracking and refinement process encountering the bouy's motion by wave. Utilizing the EKF algorithm, a minor loss in the received channel gain is observed as the sea state surpasses level 4. However, a distinct improvement is evident when compared to the fixed beamforming method. In **Fig. 6 (b)**, where the sea state level set to 8, we compare the received channel gain as the beam width is narrower (i.e., the number of antennas is increased.) When employing a Kalman-based beam tracking approach, it was observed that the performance was significantly improved by over 4 times compared to using only the initial beam. This improvement was particularly pronounced when encountering substantial variations in wave conditions. Notably, for the number of antennas 5, the algorithmic utilization and non-utilization yielded performance disparities exceeding 10 times. This discrepancy is attributed to the fact that when the beamwidth is narrow, the beam may possess favorable gain characteristics when received, but due to its limited coverage, instances of failure to intercept the signal result in diminished gain. Nevertheless, with proficient tracking performance, even with a narrow beamwidth, satisfactory signal reception can be ensured, resulting in improved gain characteristics. Hence,

the conclusion drawn from **Fig. 6** underscores the indispensability and significance of accurate motion estimation and consequent beam adjustment to ensure resilience under challenging wave conditions for the desired link quality assurance. We have compiled the detailed performance results in **Table 2** to provide a clear and comprehensive representation of the data.

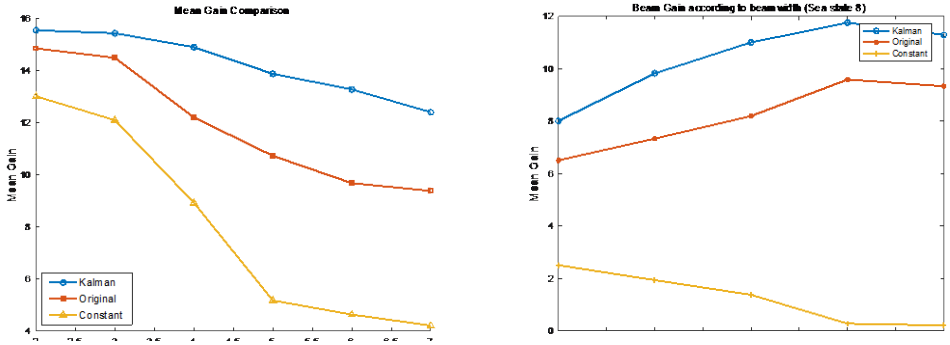

Fig. 6. Average received channel gain over time intervals for various beamforming methods: **(a)** Across a range of Sea States from 2 to 7, **(b)**. when the increasing number of antenna from 2 to 6 when operating at Sea State 8.

Table 2. Numerical results

Sea state	Method	Channel Gain	Performance Improvement
2	Fixed Beam	13.2	
2	Kalman-based	15.1	+14.4%
2	EKF-based	15.8	+19.7%
4	Fixed Beam	8.8	
4	Kalman-based	12.3	+39.77%
4	EKF-based	15.2	+72.73%
6	Fixed Beam	4.4	
6	Kalman-based	9.7	+120.5%
6	EKF-based	13.8	+245.45%

Fig. 7 shows that the difference in performance between these strategies was minimal in scenarios with minimal wave disturbance (sea state 2). However, the Kalman-based algorithm was slightly ahead of the others, showing resilience even in stable conditions. The simulation result of Sea State 8 shows that the difference was more pronounced in more turbulent sea conditions. Relying solely on the single selected beam resulted in a sharp decrease in normalized gain, approaching 0.05, increasing the probability of outages. In contrast, the strategy based on Kalman information consistently delivered superior results. These results highlight the effectiveness of Kalman-based beam adjustment techniques for receive beamforming, ensuring robust maritime communications with the movement of buoy, especially in dynamic sea states.

5. Conclusion

In this paper, we address the limitations of conventional maritime communication by modeling the dynamic maritime channel and designing adaptive beamforming strategies using Kalman-based buoy motion tracking. We first delved into the mathematical representation of the

maritime channel, juxtaposing it with actual measured data. After analyzing the simulated channel, the received beam gain at ocean surface buoys was verified. We assessed the

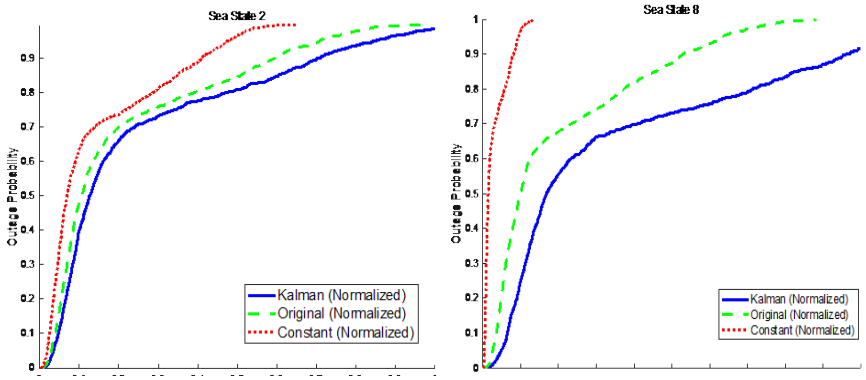

Fig. 7. Compare outage probability performance with algorithms at Sea State 2,8

similarity from the perspective of actual data-based beam gain to justify the modeling. By leveraging the anticipated wave motions, we employed the EKF to project future angles of the buoy, devising beamforming strategies that adapt to dynamic marine conditions. We proposed a Kalman-based beamformer that tracks marine motion. Our methodology centered on dynamic maritime channel modeling and the application of a Kalman-oriented buoy movement tracking system for refined beamforming. This was all in pursuit of bolstering the quality of the communication link. The simulated scenarios, taking realistic wave actions into account, underscored the heightened link quality attained through our refined beamforming approach, even amid obstacles such as turbulent waves and fluctuating sea conditions. This enhancement is markedly pronounced in maritime contexts dominated by elevated sea conditions. In conclusion, the advancements showcased in our research augur well for a transformative shift in the realm of maritime communication applications in the foreseeable future.

Acknowledgement

This research was a part of the project titled 'The advancement of smart aids to navigation facilities (20210636)', funded by the Ministry of Oceans and Fisheries, Korea.

References

[1] J. H. Sung, S. Y. Cho, W. G. Jeon, K. W. Park, S. J. Ahn and K. W. Kwon, “MIMO-aided Efficient Communication Resource Scheduling Scheme in VDES,” *KSII Transactions on Internet and Information Systems*, vol.16, no.8, pp.2736–2750, 2022. Article (CrossRef Link)

[2] H. C. Lee, H. H. Song, S. Y. Cho, K. W. Kwon, S. H Park and T. H. Im, “High-Speed Maritime Object Detection Scheme for the Protection of the Aid to Navigation,” *KSII Transactions on Internet and Information Systems*, vol. 16, no. 2, pp.692–712, 2022. Article (CrossRef Link)

[3] D. Palma, “Enabling the Maritime Internet of Things: CoAP and 6LoWPAN Performance Over VHF Links,” *IEEE Internet of Things Journal*, vol.5, no.6, pp.5205-5212, 2018. Article (CrossRef Link)

[4] T. Yang, Z. Zheng, H. Liang, R. Deng, N. Cheng and X. Shen, “Green Energy and Content-Aware Data Transmissions in Maritime Wireless Communication Networks,” *IEEE Transactions on Intelligent Transportation Systems*, vol.16, no.2, pp.751-762, 2015. Article (CrossRef Link)

[5] Z. Sun, X. Hu, Y. Qi, Y. Huang and S. Li, "Mcmod: the multi-category large-scale dataset for maritime object detection," *Computers, Materials & Continua*, vol.75, no.1, pp.1657-1669, 2023. Article (CrossRef Link)
[6] C. Lu, M. Zhao, I. Khan and P. Uthansakul, "Prospect Theory Based Hesitant Fuzzy Multi-Criteria Decision Making for Low Sulphur Fuel of Maritime Transportation," *Computers, Materials & Continua*, vol.66, no.2, pp.1511-1528, 2021. Article (CrossRef Link)
[7] J. Wang et al., "Wireless Channel Models for Maritime Communications," *IEEE Access*, vol.6, pp.68070-68088, 2018. Article (CrossRef Link)
[8] R. Duan, J. Wang, H. Zhang, Y. Ren and L. Hanzo, "Joint Multicast Beamforming and Relay Design for Maritime Communication Systems," *IEEE Transactions on Green Communications and Networking*, vol.4, no.1, pp.139-151, 2020. Article (CrossRef Link)
[9] A. Kaewpukdee and P. Uthansakul, "Characteristic of Line-of-Sight in Infrastructure-to-Vehicle Visible Light Communication using MIMO Technique," *Computers, Materials & Continua*, vol.74, no.1, pp.1025-1048, 2022. Article (CrossRef Link)
[10] D. Kidston and T. Kunz, "Challenges and opportunities in managing maritime networks," *IEEE Communications Magazine*, vol.46, no.10, pp.162-168, 2008. Article (CrossRef Link)
[11] S. Blandino, J. Senic, C. Gentile, D. Caudill, J. Chuang and A. Kayani, "Markov Multi-Beamtracking on 60 GHz Mobile Channel Measurements," *IEEE Open Journal of Vehicular Technology*, vol.3, pp.26-39, 2022. Article (CrossRef Link)
[12] S. Kutty and D. Sen, "Impact of Intra-Cluster Angular Spread on the Performance of NLoS Millimeter Wave Links With Imperfect Beam Alignment," *IEEE Transactions on Vehicular Technology*, vol.69, no.2, pp.1813-1827, 2020. Article (CrossRef Link)
[13] E. Karipidis, N. D. Sidiropoulos, and Z.-Q. Luo, "Quality of Service and Max-Min Fair Transmit Beamforming to Multiple Cochannel Multicast Groups," *IEEE Transactions on Signal Processing*, vol.56, no.3, pp.1268-1279, 2008. Article (CrossRef Link)
[14] S. Ali, A. Jalal, M. H. Alatiyyah, K. Alnowaiser and J. Park, "Vehicle Detection and Tracking in UAV Imagery via YOLOv3 and Kalman Filter," *Computers, Materials & Continua*, vol.76, no.1, pp.1249-1265, 2023. Article (CrossRef Link)
[15] H. Zhang, G. Yang, H. Yu and Z. Zheng, "Kalman Filter-Based CNN-BiLSTM-ATT Model for Traffic Flow Prediction," *Computers, Materials & Continua*, vol.76, no.1, pp.1047-1063, 2023. Article (CrossRef Link)
[16] M. Pervaiz, M. Shorfuzzaman, A. Alsufyani, A. Jalal, S. A. Alsuhibany and J. Park, "Tracking and Analysis of Pedestrian's Behavior in Public Places," *Computers, Materials & Continua*, vol.74, no.1, pp.841-853, 2023. Article (CrossRef Link)
[17] S. Alabed, M. Al-Rabayah and W. H. Fouad Aly, "A Beamforming Technique Using Rotman Lens Antenna for Wireless Relay Networks," *Computers, Materials & Continua*, vol.73, no.3, pp.5641-5653, 2022. Article (CrossRef Link)
[18] N. H. Jeong, M. Kim, J.H. Choi and K. T. Kim, "Beam Scheduling of Maritime Multifunctional Radar Based on Binary Integration," *IEEE Access*, vol.11, pp.35796-35807, 2023. Article (CrossRef Link)
[19] F. S. Alqurashi, A. Trichili, N. Saeed, B. S. Ooi and M. S. Alouini, "Maritime Communications: A Survey on Enabling Technologies, Opportunities, and Challenges," *IEEE Internet of Things Journal*, vol.10, no.4, pp.3525-3547, 2023. Article (CrossRef Link)
[20] L. H. Holthuijsen, "Description of ocean waves," *Waves in Oceanic and Coastal Waters*, 1st ed., vol. 1, pp.24-55, 2007. Article (CrossRef Link).
[21] Y. Huo, X. Dong and S. Beatty, "Cellular Communications in Ocean Waves for Maritime Internet of Things," *IEEE Internet of Things Journal*, vol.7, no.10, pp.9965-9979, 2020. Article (CrossRef Link)
[22] R. Cao, B. Liu, F. Gao and X. Zhang, "A Low-Complex One-Snapshot DOA Estimation Algorithm with Massive ULA," *IEEE Communications Letters*, vol.21, no.5, pp.1071-1074, 2017. Article (CrossRef Link)

[23] J. Bao and H. Li, "Motion Aware Beam Tracking in Mobile Millimeter Wave Communications: A Data-Driven Approach," in *Proc. of ICC 2019 - 2019 IEEE International Conference on Communications (ICC)*, pp.1-6, 2019. Article (CrossRef Link)
[24] Y. Sim, S. Sin, J. Cho, S. Moon, Y. You, C. H. Kim and I. Hwang, "Beam Tracking Method Using Unscented Kalman Filter for UAV-Enabled NR MIMO-OFDM System with Hybrid Beamforming," *KSII Transactions on Internet and Information Systems*, vol.17, no.1, pp.280-294, 2023. Article (CrossRef Link)

Kyeongjea Lee received the B.S. degrees from the School of Electronic Engineering, Gachon, Gyeonggi, South Korea, in 2018. He is currently working toward the Ph.D. degree at the Electrical and Electronic Engineering, Yonsei University, Seoul, South Korea. His research interests include the advanced MIMO technologies for wireless communication systems.

Joo-Hyun Jo (Student Member, IEEE) received the B.S. degree in Electronic Convergence Engineering from Kwangwoon University, Seoul, South Korea, in 2015. He is currently working toward the Ph.D. degree at the Electrical and Electronic Engineering, Yonsei University, Seoul, South Korea. His research interests include the advanced MIMO technologies for 5G vehicular use cases and wireless communication systems.

Sungyoon Cho received the B.S., M. S. and Ph.D. degrees in electrical and electronic engineering from Yonsei University, Seoul, Korea, in 2006, 2008, and 2013, respectively. From 2013 to 2020, he was with Samsung Electronics, Korea, as a Staff Engineer to research cellular communication systems and develop 4G and 5G modem chipset. Since 2020, he has been with Korea Electronics Technology Institute (KETI) as a Principal Researcher to develop the advanced technologies for embedded network. His research interests are in the fundamental aspects of wireless communication and signal processing and learning algorithms for practical application.

Kiwon Kwon received B.S. and M.S. degrees in computer engineering from Kwangwoon University, Korea, in 1997 and 1999, He also received the Ph.D. degree in the School of Electrical & Electronics Engineering from Chung-Ang University, Korea, in 2011. In 1999, he joined in KETI, Korea, where he is currently a Group Leader with Oceans and Fisheries ICT Group. His research interests are in the area of advanced broadcasting/communication system, digital twin, oceans and fisheries ICT.

Dong Ku Kim (Senior Member, IEEE) has been a professor at the School of Electrical and Electronic Engineering, Yonsei University, since 1994. He is a chair of the governing board of the public-priavate Open RAN Industry Alliance in Korea. He is also a member of the special committee for national strategic technology under the presidential advisory council on S&T. He served as a chair of the publicprivate 5G Forum executive committee over the last ten years and a member of the 5G+ strategy committee chaired by the minister of the Ministry of Science and ICT minister (MSIT). He received the Yellow Stripes of the Order of Service Merit from the Korean government for the contribution of the world's first commercialization of 5G, ecosystem creation, and the defusion of convergence among 5G-based industries in April 2020. He received IEEE Communication Society Career Award for Public Service in the Field of Telecommunication on Dec.2020. He received his Ph.D. from the University of Southern California, Los Angeles, in 1992. He worked on CDMA systems in the cellular infrastructure group of Motorola at Fort Worth, Texas. His current research interests are the advanced MIMO for 5G vehicular use cases, RSMA for future mobile systems, smart buoy energy efficient transmission, and Open RAN.